ELSEVIER

Journal of Biomechanics 37 (2004) 205–212

JOURNAL OF BIOMECHANICS

www.elsevier.com/locate/jbiomech
www.JBiomech.com

Structural behavior of human lumbar spinal motion segments

Mack G. Gardner-Morse*, Ian A.F. Stokes

Department of Orthopaedics and Rehabilitation, University of Vermont, Stafford Hall, Burlington, VT 05405-0084, USA

Accepted 20 October 2003

Abstract

The objectives of this study were to obtain linearized stiffness matrices, and assess the linearity and hysteresis of the motion segments of the human lumbar spine under physiological conditions of axial preload and fluid environment. Also, the stiffness matrices were expressed in the form of an 'equivalent' structure that would give insights into the structural behavior of the spine. Mechanical properties of human cadaveric lumbar L2-3 and L4-5 spinal motion segments were measured in six degrees of freedom by recording forces when each of six principal displacements was applied. Each specimen was tested with axial compressive preloads of 0, 250 and 500 N. The displacements were four slow cycles of ± 0.5 mm in anterior–posterior and lateral displacements, ± 0.35 mm axial displacement, $\pm 1.5^\circ$ lateral rotation and $\pm 1^\circ$ flexion-extension and torsional rotations. There were significant increases with magnitude of preload in the stiffness, hysteresis area (but not loss coefficient) and the linearity of the load-displacement relationship. The mean values of the diagonal and primary off-diagonal stiffness terms for intact motion segments increased significantly relative to values with no preload by an average factor of 1.71 and 2.11 with 250 and 500 N preload, respectively (all eight tests $p<0.01$). Half of the stiffness terms were greater at L4-5 than L2-3 at higher preloads. The linearized stiffness matrices at each preload magnitude were expressed as an equivalent structure consisting of a truss and a beam with a rigid posterior offset, whose geometrical properties varied with preload. These stiffness properties can be used in structural analyses of the lumbar spine.

Keywords: Lumbar spine; Motion segment; Stiffness matrix; Finite element analysis

1. Introduction

The mechanical function of the spine is the summation of the behavior of its individual motion segments, where a motion segment is a structural unit of the spine consisting of two vertebrae and the intervening soft tissues (Fig. 1). Motion segment behavior is a key component of biomechanical analyses of the spine, including analyses of spinal loading (Stokes and Gardner-Morse, 2001), dynamics of injury (Kasra et al., 1992; Pankoke et al., 2001), spinal stability (Bergmark, 1989; Cholewicki and McGill, 1996; Gardner-Morse et al., 1995; Gardner-Morse and Stokes, 1998), and simulations of surgery (Aubin et al., 2003; Stokes and Gardner-Morse, 1993).

Isolated tests of motion segment behavior in individual degrees of freedom provide information that is specific to those degrees of freedom and cannot be generalized to three-dimensional analyses because of the interaction between degrees of freedom, called 'coupling' (Panjabi et al., 1976). A 6×6 stiffness or flexibility matrix is needed to describe how forces displace a vertebra relative to its fixed neighbor (Panjabi et al., 1976).

In general a 6×6 stiffness matrix has 36 terms. The number of independent stiffness matrix terms is reduced to 21 by consideration of matrix symmetry required by conservation of energy if the material properties are linear. Matrix symmetry results in complementary pairing of off-diagonal terms hence $k_{12}=k_{21}$, etc., in Fig. 2. Sagittal plane symmetry requires that nine of the 21 terms are zero (terms for forces expected to be zero for displacements within the sagittal plane, e.g. no lateral force associated with axial compression, hence k_{13} and $k_{31}=0$, etc.). This leaves 12 nonzero stiffness

*Corresponding author. Tel.: +1-802-656-2250; fax: +1-802-656-4247.

E-mail address: mack.gardner-morse@uvm.edu (M.G. Gardner-Morse).

0021-9290/$ - see front matter © 2003 Elsevier Ltd. All rights reserved.
doi:10.1016/j.jbiomech.2003.10.003

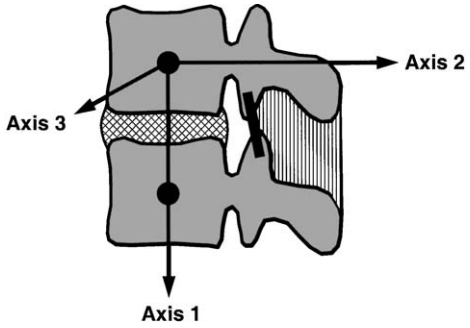

Fig. 1. Motion segment considered as a 2-node element. Nodes are at vertebral body centers. The axis numbering convention follows that normally used in finite element analyses. The lower vertebra was constrained during the tests while displacements were applied to the upper vertebra.

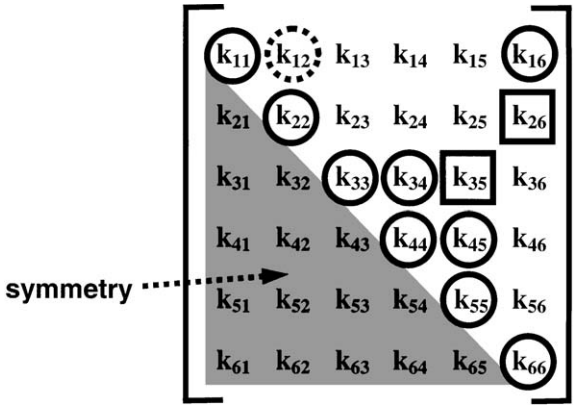

Fig. 2. Terms in the motion segment stiffness matrix. The six diagonal terms are those stiffness terms that relate forces or moments to the co-linear displacements or rotations. There is symmetry about the diagonal of the off-diagonal terms (in the shaded area), hence $k_{53}=k_{35}$, etc. The un-marked terms are expected to be zero based on sagittal plane motion segment symmetry. The terms k_{35} and k_{26} (marked by squares) are those identified by Goel (1987) as "primary" off-diagonal terms. The other three circled off-diagonal terms are associated with an antero-posterior offset of the structural axis from the vertebral body centers. The dashed circle identifies the coupling term (axial compression, anterior shear) that was found not to be significantly different from zero. Degrees of freedom 1–3 correspond to translations, and 4–6 correspond to rotations, with the sequence indicated in Fig. 1.

terms (Fig. 2). Goel (1987) defined a simplified stiffness matrix for the motion segment with six diagonal terms (relating co-linear displacements or rotations) and two "primary" off-diagonal terms, assuming that the motion segment had beam-like behavior. The two primary off-diagonal terms relate the anterior–posterior (A–P) shear forces to the applied flexion-extension rotations (or the complementary flexion-extension moments to A–P shear displacements) and lateral shear forces with lateral bending rotations (or the complementary lateral bending moments to lateral shear displacements). This beam-like behavior requires that the motions segment's axis system be aligned with its structural axis.

Since the motion segment has two vertebrae, each having six degrees of freedom, it requires a 12×12 stiffness matrix. This matrix can be derived from the 6×6 matrix for one vertebral center moving relative to a fixed adjacent vertebra, by using the principle of force equilibrium, compatible with the specified distance between the two vertebral centers (Gardner-Morse et al., 1990).

A shear beam with a rigid A–P offset was proposed by Gardner-Morse et al. (1990) as an approximate representation of an experimental stiffness matrix. This 'equivalent' beam has seven independent parameters, compared with up to 12 terms in the experimental stiffness matrix (Fig. 2). In this paper we propose an extension of that method, that also includes a truss element, thus permitting a closer approximation to the experimental data.

There are several limitations of the existing human motion segment experimental stiffness data, such that they probably do not accurately represent in vivo behavior. Most reported data do not include all six degrees of freedom (Berkson et al., 1979; Nachemson et al., 1979; Schultz et al., 1979), were obtained without physiological levels of axial compression and were performed with the specimen not surrounded by physiological isotonic fluid (e.g. Panjabi et al., 1976). Physiological axial compressive preload is known to increase stiffness by a factor of two or more (Edwards et al., 1987; Janevic et al., 1991; Gardner-Morse and Stokes, 2003) and may reduce the amount of load-displacement nonlinearity (Janevic et al., 1991; Gardner-Morse and Stokes, 2003). Discs in a physiological saline bath have greater hydration than discs that are just exposed to saline spray and wrap (Pflaster et al., 1997), and this increased hydration affects the disc biomechanics (Race et al., 2000; Costi et al., 2002). The increased hydration may also increase the repeatability of the load-displacement behavior with slow cyclic loading (Gardner-Morse and Stokes, 2003).

This paper reports the stiffness matrix and other properties of human lumbar motion segments tested with slow-rates of displacement, to obtain the quasi-static stiffness response of the motion segments, and with small displacements, to approximate the assumption of linear load-displacement behavior.

The purposes of the study were:

1. Quantify the effects of 0, 250 and 500 N axial compressive preload on the motion segment stiffness matrix, and on the hysteresis and linearity of the load-displacement relationship. The effect of preload was determined for intact motion segments and in isolated intervertebral discs.
2. Examine whether the stiffness matrix terms correlated with physical dimensions of the motion

segments, and compare the behavior of L2-3 and L4-5 segments.
3. Analyze the derived stiffness matrices at the three magnitudes of axial compressive preload to obtain the geometrical properties of an equivalent structure that included a truss and a beam element with a rigid posterior offset.

2. Methods

The load-displacement behavior of eight human lumbar motion segments (L2-3 and L4-5 from each of four human females, aged 17, 21, 52 and 58 years) was recorded directly in six degrees of freedom (6-DOF) by a Stewart platform (i.e. a 'hexapod' robot) (Stokes et al., 2002). These motion segments were dissected from human spines that had been stored at −80°C. Each specimen was radiographed and no evidence of anatomical abnormality or gross degeneration was observed. Some osteophytes were observed on the older specimens. Prior to testing, each specimen was thawed, embedded in end-fittings using PMMA, and radiographed to identify the position of the vertebral body centers that in turn defined the axis-system for testing as described in Stokes et al. (2002). During testing, specimens were immersed in an isotonic saline bath to simulate the physiological environment. The bath was cooled to approximately 4°C to minimize tissue changes over the period of testing.

Each test was performed with axial compressive preloads of 0, 250 and 500 N applied in a varied sequence. The non-zero preload magnitudes represent spinal loading during standing and sitting (Andersson et al., 1984). The specimen was allowed to equilibrate with each preload for at least 3 h before the load-displacement tests. Six tests (three pure translations and three pure rotations) were sequentially performed with four sawtooth-waveform cycles of 87 s in each displacement direction. The applied displacements and resulting forces were recorded at 1 Hz. The displacements were ±0.5 mm in the A–P and lateral directions, ±0.35 mm in the axial direction, ±1.5° in lateral bending rotation and ±1° in flexion-extension and torsional rotations. These magnitudes of displacement were selected to be compatible with the linearizing assumptions made in subsequent analyses and were about 20% of the reported physiological range of segmental motion (Marras et al., 1995). After testing each intact specimen, the facets and ligaments (posterior elements) were removed and the tests were repeated.

The size of each disc (lateral width, antero-posterior width and disc height) and the distance between vertebral body centers was measured from radiographs, with compensation for radiographic magnification.

The 36 independent terms of the 6 × 6 stiffness matrix and six force offset terms were estimated using a least-squares fit to the experimental data by the method reported in Stokes et al. (2002). The off-diagonal matrix terms were averaged to make the matrix symmetric.

The linearity of each load-displacement relationship was measured by subtracting the linear regression coefficient of determination (R^2) and the pure error estimate from unity (Gardner-Morse and Stokes, 2003). The hysteresis area was calculated as the enclosed area of each cycle averaged over the second and third cycles in the load-displacement recording. These two cycles were used to avoid discontinuities that could be present at the start of the first and the end of the fourth cycles. Additionally, the loss coefficient (a measure of hysteresis with strain) for the diagonal degrees of freedom was evaluated as:

$$\eta = \frac{W_d}{\pi k x_{\max}^2},$$

where η is the dimensionless loss coefficient, W_d is the hysteresis area, k is the stiffness and $x_{\max}$ is the maximum displacement (Thomson, 1972).

The eight geometrical properties of the equivalent structure consisting of a truss and a shear beam with a rigid posterior offset as illustrated in Fig. 3 were calculated using a nonlinear least squares to minimize the sum of squared differences between the equivalent structure stiffness and the experimental stiffness terms, divided by the experimental stiffness terms. The nonlinear least squares was performed using the *leastsq* routine in Matlab (The MathWorks, Inc., Natick, MA, USA). The length of the truss and the beam were assigned a value equal to the mean measured distance between vertebral body centers (36.27 mm) and the material properties were assigned arbitrary values:

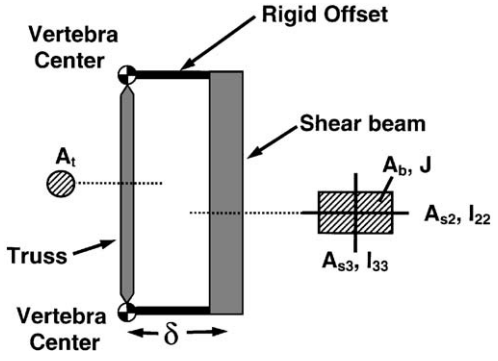

Fig. 3. Sagittal plane view of a structure consisting of a shear beam with rigid offsets and a truss and that was used to represent the empirically determined lumbar motion segment stiffness at each preload level. Properties: modulus $E = 1000\,\mathrm{N/mm^2}$, Poisson's ratio $v = 0.49$, distance between vertebral centers = 36.27 mm; A_t = truss area, A_b = beam axial area, A_{S2} and A_{S3} = beam shear areas, J, I_{22} and I_{33} = beam 2nd moments of area, δ = rigid offset.

modulus $E = 1000\,\mathrm{N/mm^2}$ and Poisson's ratio $v = 0.49$. The eight equivalent structure geometrical properties were calculated for the mean stiffness matrices at each preload.

Statistical methods were applied to determine:

1. Correlations of the diagonal terms of the stiffness matrix with specimen dimensions (by linear regression analysis);
2. Level differences between L2-3 and L4-5 (by repeated-measures ANOVAs);
3. Stiffness matrix terms that were significantly different from zero (by two-sided t-tests);
4. Differences with axial compressive preload magnitude in the diagonal and primary off-diagonal (as defined by Goel, 1987) stiffness terms. These effects were analyzed using repeated-measures ANOVAs. Significant preload effects were further analyzed with linear and quadratic contrasts.

Additionally, preload effects on the linearity, hysteresis area and the loss coefficient of the load-displacement relationships were examined.

3. Results

Experimental values of all the stiffness matrix terms that were expected to be zero (based on motion segment symmetry) were not significantly different from zero. Additionally, the axial/A–P shear coupling term (k_{12} in Fig. 2) was not significantly different from zero. This left six diagonal and five off-diagonal independent terms for consideration (Fig. 2). Increased axial compressive preloads produced progressively increased stiffness (Table 1) as found previously for porcine motion segments (Stokes and Gardner-Morse, 2003). The mean values of the diagonal and primary off-diagonal stiffness terms for intact motion segments increased significantly relative to values with no preload by an average factor of 1.71 and 2.11 with 250 and 500 N preload, respectively (all eight tests $p<0.01$). Preload had the greatest effect on axial stiffness with factors of 3.88 and 5.53 with 250 and 500 N compression, respectively (Table 1). The linear trend of increasing stiffness with preload was highly significant ($p<0.01$). The increase in stiffness with preload was observed to be greater for the preload increase from 0 to 250 N than for the preload increase from 250 to 500 N, but statistically the quadratic trend was only significant for A–P shear and primary off-diagonal stiffnesses.

There were no consistent correlations between stiffness values and the linear dimensions of the specimens, although the correlation coefficients were observed to be predominantly negative (i.e. larger specimens were less stiff). The average dimensions of the specimens were 36.3 mm (33.0–39.8 mm) between vertebral centers; 45.5 mm (41.2–58.1 mm) disc lateral width, 32.5 mm (30.0–34.7 mm) A–P width and 8.9 mm (6.4–10.3 mm) disc height.

While there were no significant difference by anatomical level (L2-3 compared with L4-5) with zero preload, some terms were significantly different at 250 and 500 N preload (Table 1). At 250 N preload, 5 of the 11 significant terms were different between the two anatomical levels. At 500 N preload, one additional term was different by level. These significant differences by level ranged from 10.3% to 50.1%.

Removal of the posterior elements (facets and ligaments) significantly decreased all of the stiffness terms except for axial stiffness, at all levels of axial compressive preload (Table 2). The mean stiffness of the diagonal terms (excluding axial stiffness) was 21%, 28% and 32% of the intact stiffness at 0, 250 and 500 N preload, respectively. The largest decrease in stiffness with removal of the facets was in torsion—the stiffness of the disc alone was 9%, 14% and 16% of the intact motion segment torsional stiffness with 0, 250 and 500 N preload, respectively. For the disc-only specimens, all eight stiffness terms increased significantly by an average factor of 2.50 and 3.48 with 250 and 500 N axial compressive preload, respectively ($p<0.01$). There were no significant level differences for the diagonal and primary off-diagonal terms in the isolated discs at any of the preloads.

The linearity of load-displacement relationships was characterized by R^2 values in the range 0.868–0.999. When R^2 values were averaged for the eight (diagonal and primary off-diagonal) terms in the stiffness matrix, the mean R^2 increased with axial compression in intact motion segments (mean $R^2 = 0.934$, 0.953 and 0.958 at 0, 250 and 500 N preload, respectively). The same effect was observed in isolated discs (mean $R^2 = 0.949$, 0.981 and 0.987 at 0, 250 and 500 N preload, respectively). The increase was significant for A–P and lateral shear relationships, and the A–P shear/flexion-extension off-diagonal load-displacement relationship in the intact motion segments. The increase was significant for the flexion-extension, axial torsion and the A–P shear/flexion-extension off-diagonal load-displacement relationships in the isolated discs.

The hysteresis appeared to be very consistent between consecutive displacement cycles (see Fig. 4). The mean hysteresis areas for intact motion segments increased significantly by 1.31 and 1.67 with 250 and 500 N axial compressive preload, respectively. Further, there were significant correlations between hysteresis area and stiffness, as reported previously for porcine motion segments (Gardner-Morse and Stokes, 2003). However, when the hysteresis was expressed as loss coefficient (i.e. divided by the maximum strain energy) the effect of preload was not evident. The mean values of the loss

Table 1
Stiffness ± SE of intact motion segments with 0, 250 and 500 N axial compressive preload

	Level	Δ_1	Δ_2	Δ_3	Δ_4	Δ_5	Δ_6
Axial compressive preload at 0 N (mean of L2-3 and L4-5)							
F_1		438 ± 92					−1370 ± 519
F_2			251 ± 42				6510 ± 969
F_3				332 ± 64	11,000 ± 2000	−6960 ± 1100	
F_4					564,000 ± 89,000	−235,000 ± 38,200	
F_5			(Symmetric)			174,000 ± 20,500	
F_6							241,000 ± 33,100
Axial compressive preload at 250 N							
F_1	L2-3	1700 ± 67[a]					−4280 ± 1130[a]
	L4-5						
F_2	L2-3		346 ± 63				8340 ± 1240
	L4-5		389 ± 76				10,200 ± 1790
F_3	L2-3			447 ± 68[a]	12,100 ± 1740[a]	−9360 ± 971[a]	
	L4-5						
F_4	L2-3				668,000 ± 144,000	−250,000 ± 34,200[a]	
	L4-5				744,000 ± 137,000		
F_5	L2-3		(Symmetric)			211,000 ± 17,900	
	L4-5					301,000 ± 29,900	
F_6	L2-3						266,000 ± 33,000
	L4-5						467,000 ± 80,500
Axial compressive preload at 500 N							
F_1	L2-3	2420 ± 158[a]					−5180 ± 1940[a]
	L4-5						
F_2	L2-3		397 ± 68				9000 ± 1330
	L4-5		473 ± 78				11,100 ± 2160
F_3	L2-3			523 ± 73[a]	13,400 ± 1890[a]	−10,400 ± 1760	
	L4-5					−11,600 ± 1250	
F_4	L2-3				734,000 ± 170,000	−272,000 ± 33,500[a]	
	L4-5				832,000 ± 129,000		
F_5	L2-3		(Symmetric)			236,000 ± 12,900	
	L4-5					377,000 ± 44,800	
F_6	L2-3						287,000 ± 27,000
	L4-5						575,000 ± 137,000

Units are N, mm and rad. Δ_1 through Δ_3 are translations and Δ_4 through Δ_6 are rotations in the sequence indicated in Figs. 1 and 2. Similarly, F_1 through F_3 are the three forces and F_4 through F_6 are the three torques. Stiffness values are tabulated in the format of the stiffness matrix for the upper vertebra center relative to the fixed lower vertebra. Where values for L2-3 and L4-5 were significantly different, separate values are given. *Note*: There were no level differences with 0 N preload.

[a] Not significantly different by lumbar level and is a mean of L2-3 and L4-5.

Table 2
Diagonal and primary off-diagonal stiffness matrix terms of isolated discs, expressed as a percent of the stiffness of intact motion segments

Preload (N)	k_{11} (%)	k_{22} (%)	k_{33} (%)	k_{44} (%)	k_{55} (%)	k_{66} (%)	k_{35} (%)	k_{26} (%)
0	92.5 ± 12.0	23.0 ± 6.3	22.5 ± 4.3	8.6 ± 2.2	30.2 ± 6.8	20.8 ± 6.5	20.3 ± 4.6	19.5 ± 5.4
250	100.6 ± 5.1	30.6 ± 3.7	31.5 ± 3.6	13.7 ± 1.8	43.3 ± 9.6	20.7 ± 2.8	33.2 ± 4.8	25.7 ± 3.7
500	104.9 ± 3.9	34.5 ± 3.3	35.6 ± 2.9	16.4 ± 1.7	49.6 ± 8.9	25.7 ± 4.1	38.1 ± 4.0	34.1 ± 5.7

Values given are the mean ± SE for all eight motion segments.

coefficient for the six diagonal terms for intact motion segments (averaged over specimens and preloads) were 0.104, 0.123, 0.091, 0.125, 0.112 and 0.123.

In intact motion segments, it was observed that there was an apparently bilinear load-displacement relationship about zero displacement for flexion-extension, A–P shear and axial displacement (Fig. 4). The average ratios of the larger to the smaller of the stiffness values for compression-tension, P–A shear and extension-flexion were 2.70, 2.40 and 3.11. These directional differences were observed at all three levels of preload, although they became slightly smaller with increased preload. This bilinear behavior was not evident in isolated discs for A–P shear and flexion-extension (Fig. 4). The

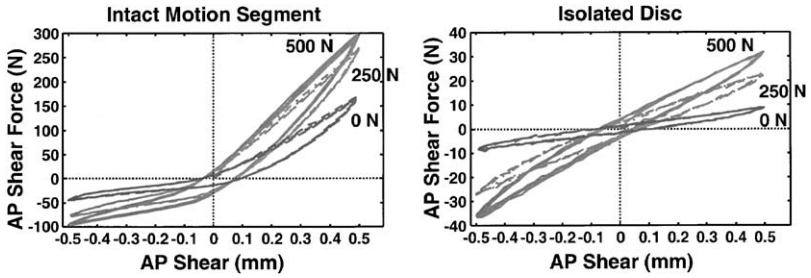

Fig. 4. A–P forces produced by A–P displacements with 0, 250 and 500 N axial preload for four cycles of 'sawtooth' displacement for an intact motion segment (left) and isolated disc (right). The bilinear behavior (directional differences) evident in the intact motion segments was also observed for other displacements in the sagittal plane (axial displacement and flexion-extension). Note the repeatability over the cycles and the increase in stiffness with preload.

Table 3
Geometrical properties of the 'equivalent structure' (Fig. 3) that approximate the motion segment stiffness matrices at each preload, but not broken down by anatomical level

Compression preload (N)	Truss axial area, A_t (mm^2)	Beam axial area, A_b, (mm^2)	Beam A–P shear area, A_{s2} (mm^2)	Beam lateral shear area, A_{s3} (mm^2)	Beam torsional constant, J (mm^4)	Beam lateral inertia, I_{22} (mm^4)	Beam flexion-extension inertia, I_{33} (mm^4)	Beam rigid offset, δ (mm)
0	14.39	1.484	45.00	115.73	18141	2103.0	3663.6	33.47
250	55.97	5.785	74.59	108.99	39153	3597.2	4161.1	26.85
500	80.21	7.425	82.61	120.08	45996	4463.4	5143.9	25.29

directional differences in stiffness for A–P shear and flexion-extension were less in isolated discs than in intact motion segments in 23 of 24 cases (8 motion segments at three levels of preload).

The equivalent structure (Fig. 3) matched four diagonal and one off-diagonal stiffness terms exactly. The differences between the remaining stiffness terms were between −12.4% and 25.3% at 0 N preload, between −11.8% and 22.7% at 250 N preload and between −9.5% and 15.4% at 500 N preload. The equivalent structure parameters having the greatest differences at differing preloads were the truss area (A_t) (increase of 5.6 times from 0 to 500 N preload), the axial area of the beam (A_b) (increase of 5.0 times from 0 to 500 N preload), and the torsional constant (J) (increase of 2.5 times from 0 to 500 N preload) (Table 3). The beam posterior rigid offset (δ) was relatively constant (25–34 mm) at differing preloads. The least-squares method did not reliably calculate best fit parameters of the equivalent structure for the individual anatomical levels (L2-3 and L4-5), hence values in Table 3 correspond to the pooled data from both anatomical levels.

When the stiffness matrices of the isolated disc were examined, all three matrix terms associated with a sagittal plane offset were not significantly different from zero for L2-3 and only the lateral shear/torsion coupling term for L4-5 was significantly different from zero at all of the preloads. This was expected, since the structural axis of the disc alone was expected to be more closely aligned with the vertebral centers.

4. Discussion

The load-displacement behavior of human lumbar motion segments was found to depend on the magnitude of the axial compressive preload. Preload increased the stiffness, linearity of the load-displacement behavior, and hysteresis area, but not loss coefficient. These findings indicate that motion segment stiffness, linearity and hysteresis measured without preloads underestimate the in vivo values in all degrees of freedom. These effects were present in both intact motion segments and in isolated intervertebral discs. The stiffness values and changes with axial compressive preload found in this study were similar to previous studies (Edwards et al., 1987; Janevic et al., 1991; Gardner-Morse and Stokes, 2003). The increase in hysteresis with preload was similar to that found in porcine motion segments (Gardner-Morse and Stokes, 2003). However, this effect of preload was not evident in the loss coefficient. Loss coefficient is the hysteresis area normalized by the maximum strain energy. Because of the fluid shifts that occurred when specimens equilibrated to changes in preload, both the water content (and volume) of the

disc, as well as its loading state may have produced the observed changes in mechanical behavior.

All of the motion segment stiffness matrix terms that were expected to be zero as a result of sagittal plane symmetry had empirical values not significantly different from zero. Additionally, the stiffness term associated with coupling between axial compression and A–P shear was not significantly different from zero. The significant terms in the experimental stiffness matrices correspond to non-zero terms in the stiffness matrix of a beam with a rigid posterior offset. For the stiffness terms that differed between the two anatomical levels with 250 and 500 N preloads, L4-5 was stiffer than L2-3. Since these differences were not significant in the isolated discs, these differences were attributed to the posterior elements. No correlations of motion segment stiffnesses with physical dimensions were found, as was also reported by Berkson et al. (1979).

The equivalent structure consisting of a truss and a shear beam with a rigid posterior offset was found to be an accurate representation of the linearized stiffness matrix under the tested conditions of slow and small displacements. When the stiffness matrices of the 'equivalent' structures were calculated, the terms were within ± 0.57SD of the measured stiffness means. This structure provides insights into the physical behavior of the motion segment. While many properties showed large changes with increasing preload, it was notable that the rigid offset δ was almost constant with increasing preload. In intact motion segments the rigid offset δ represents a posterior displacement (relative to the vertebral center) of the effective structural axis of the motion segment. It was not evident for disc-only specimens, hence it was attributed to the posterior elements. The addition of a truss allows the equivalent structure to match the coupling between axial displacement/force and flexion-extension moment/rotation exactly (k_{16} in Fig. 2). Gardner-Morse et al. (1990) found that a shear beam without offsets was a good match to the thoracic flexibility matrices in Panjabi et al. (1976), suggesting that the posterior elements have a greater effect in lumbar than in thoracic motion segments.

All of the motion segment stiffnesses except for the axial stiffness decreased with the removal of posterior elements. A large decrease in torsional stiffness with the removal of the posterior elements, and lesser decreases in lateral bending and flexion and extension stiffness have been reported previously, but using greater ranges of motion than used here (Schultz et al., 1979; Stokes, 1988; Posner et al., 1982).

The observed differences in stiffness between flexion-extension and A–P shear were compatible with the expected stiffening effects of facet joint engagement and these differences were not observed after facet removal. The nonlinear behavior in compression-tension did not change with the removal of the posterior elements, so it was presumably due to the disc. Panjabi et al. (1976) presented two stiffness matrices, one for positive and one for negative displacements. This approach defines the diagonal stiffness terms for both displacement directions, but does not include all permutations of the off-diagonal terms for differing displacement directions.

The main limitation of this approach to represent the motion segment as a stiffness matrix was that it required an assumption of linear load-displacement behavior. The high R^2 values suggest that this is a reasonable assumption over the range of displacements tested here. The displacement rate used in these tests was slow, to simulate quasi-static loadings. The apparent stiffness is expected to increase at faster displacement rates. The low temperature ($\sim 4^\circ$C) may have increased the measured stiffness relative to physiological values.

The linearized stiffness matrices at each preload magnitude can be used in structural analyses of the lumbar spine. Alternatively, these stiffness matrices can be expressed as an equivalent structure consisting of a truss and a beam with a rigid posterior offset, with cross-sectional properties that vary with preload. These equivalent structures can be employed in structural spinal analyses, and the changes in spinal stiffness with preload can be used to update spinal stiffness properties as shown in Stokes and Gardner-Morse (2003).

Acknowledgements

Supported by NIH R01 AR44119. Motion segments were supplied by the Anatomical Board of the State of Texas and National Disease Research Interchange (NDRI). Dr. Richard Single performed the statistical analyses. We acknowledge helpful discussions with Dr. Jean-Guy Beliveau.

References

Andersson, G.B.J., Chaffin, D.B., Pope, M.H., 1984. Occupational biomechanics of the lumbar spine. In: Pope, M.H., Frymoyer, J.W., Andersson, G. (Eds.), Occupational Low Back Pain. Praeger, New York, pp. 45.

Aubin, C.E., Petit, Y., Stokes, I.A.F., Poulin, F., Gardner-Morse, M.G., Labelle, H., 2003. Biomechanical modeling of posterior instrumentation of the scoliotic spine. Computer Methods in Biomechanics and Biomedical Engineering 6, 27–32.

Bergmark, A., 1989. Stability of the lumbar spine. A study in mechanical engineering. Acta Orthopaedica Scandinavica Supplementum 230, 1–54.

Berkson, M.H., Nachemson, A.L., Schultz, A.B., 1979. Mechanical properties of human lumbar spine motion segments—Part II: responses in compression and shear; influence of gross morphology. Journal of Biomechanical Engineering 101, 53–57.

Cholewicki, J., McGill, S.M., 1996. Mechanical stability of the in vivo lumbar spine: implications for injury and chronic low back pain. Clinical Biomechanics 11, 1–15.

Costi, J.J., Hearn, T.C., Fazzalari, N.L., 2002. The effect of hydration on the stiffness of intervertebral discs in an ovine model. Clinical Biomechanics 17, 446–455.

Edwards, W.T., Hayes, W.C., Posner, I., White III, A.A., Mann, R.W., 1987. Variation of lumbar spine stiffness with load. Journal of Biomechanical Engineering 109, 35–42.

Gardner-Morse, M.G., Stokes, I.A.F., 1998. The effects of abdominal muscle co-activation on lumbar spine stability. Spine 23, 86–92.

Gardner-Morse, M.G., Stokes, I.A.F., 2003. Physiological axial compressive preloads increase motion segment stiffness, linearity and hysteresis in all six degrees of freedom for small displacements about the neutral posture. Journal of Orthopaedic Research 21, 547–552.

Gardner-Morse, M.G., Laible, J.P., Stokes, I.A.F., 1990. Incorporation of spinal flexibility measurements into finite element analysis. Journal of Biomechanical Engineering 112, 481–483.

Gardner-Morse, M., Stokes, I.A.F., Laible, J.P., 1995. Role of muscles in lumbar spine stability in maximum extension efforts. Journal of Orthopaedic Research 13, 802–808.

Goel, V.K., 1987. Three-dimensional motion behavior of the human spine—a question of terminology. Journal of Biomechanical Engineering 109, 353–355.

Janevic, J., Ashton-Miller, J.A., Schultz, A.B., 1991. Large compressive preloads decrease lumbar motion segment flexibility. Journal of Orthopaedic Research 9, 228–236.

Kasra, M., Shirazi-Adl, A., Drouin, G., 1992. Dynamics of human lumbar intervertebral joints. Experimental and finite-element investigations. Spine 17, 93–102.

Marras, W.S., Lavender, S.A., Leurgans, S.E., Fathallah, F.A., Ferguson, S.A., Allread, W.G., et al., 1995. Biomechanical risk factors for occupationally related low back disorders. Ergonomics 38, 377–410.

Nachemson, A.L., Schultz, A.B., Berkson, M.H., 1979. Mechanical properties of human lumbar spine motion segments; influences of age, sex, disc level, and degeneration. Spine 4, 1–8.

Panjabi, M.M., Brand, R.A., White III, A.A., 1976. Three-dimensional flexibility and stiffness properties of the human thoracic spine. Journal of Biomechanics 9, 185–192.

Pankoke, S., Hofmann, J., Wolfel, H.P., 2001. Determination of vibration-related spinal loads by numerical simulation. Clinical Biomechanics 16 (Suppl. 1), S45–S56.

Pflaster, D.S., Krag, M.H., Johnson, C.C., Haugh, L.D., Pope, M.H., 1997. Effect of test environment on intervertebral disc hydration. Spine 22, 133–139.

Posner, I., White III, A.A., Edwards, W.T., Hayes, W.C., 1982. A biomechanical analysis of the clinical stability of the lumbar and lumbosacral spine. Spine 7, 374–389.

Race, A., Broom, N.D., Robertson, P., 2000. Effect of loading rate and hydration on the mechanical properties of the disc. Spine 25, 662–669.

Schultz, A.B., Warwick, D.N., Berkson, M.H., Nachemson, A.L., 1979. Mechanical properties of human lumbar spine motion segments—Part I: responses in flexion, extension, lateral bending, and torsion. Journal of Biomechanical Engineering 101, 46–52.

Stokes, I.A.F., 1988. Mechanical function of facet joints in the lumbar spine. Clinical Biomechanics 3, 101–105.

Stokes, I.A.F., Gardner-Morse, M., 1993. Three-dimensional simulation of Harrington distraction instrumentation for surgical correction of scoliosis. Spine 18, 2457–2464.

Stokes, I.A.F., Gardner-Morse, M., 2001. Lumbar spinal muscle activation synergies predicted by multi-criteria cost function. Journal of Biomechanics 34, 733–740.

Stokes, I.A.F., Gardner-Morse, M., 2003. Spinal stiffness increases with axial load: another stabilizing consequence of muscle action. Journal of Electromyography and Kinesiology 13, 397–402.

Stokes, I.A.F., Gardner-Morse, M., Churchill, D., Laible, J.P., 2002. Measurement of a spinal motion segment stiffness matrix. Journal of Biomechanics 35, 517–521.

Thomson, W.T., 1972. Theory of Vibration with Applications. Prentice-Hall, Englewood Cliffs, NJ, p. 67.